



**HAL**  
open science

## Global 3D full-scale turbulence simulations of TCV-X21 experiments with SOLEDGE3X

H. Bufferand, G. Ciraolo, R. Düll, G. Falchetto, N. Fedorczak, Y. Marandet, V. Quadri, M. Raghunathan, N. Rivals, F. Schwander, et al.

► **To cite this version:**

H. Bufferand, G. Ciraolo, R. Düll, G. Falchetto, N. Fedorczak, et al.. Global 3D full-scale turbulence simulations of TCV-X21 experiments with SOLEDGE3X. Nuclear Materials and Energy, 2024, 41, pp.101824. 10.1016/j.nme.2024.101824 . hal-04948123

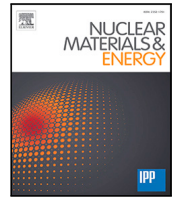
**HAL Id: hal-04948123**

**<https://hal.science/hal-04948123v1>**

Submitted on 14 Feb 2025

**HAL** is a multi-disciplinary open access archive for the deposit and dissemination of scientific research documents, whether they are published or not. The documents may come from teaching and research institutions in France or abroad, or from public or private research centers.

L'archive ouverte pluridisciplinaire **HAL**, est destinée au dépôt et à la diffusion de documents scientifiques de niveau recherche, publiés ou non, émanant des établissements d'enseignement et de recherche français ou étrangers, des laboratoires publics ou privés.



# Global 3D full-scale turbulence simulations of TCV-X21 experiments with SOLEDGE3X

H. Bufferand<sup>a,\*</sup>, G. Ciraolo<sup>a</sup>, R. Düll<sup>a</sup>, G. Falchetto<sup>a</sup>, N. Fedorczak<sup>a</sup>, Y. Marandet<sup>b</sup>, V. Quadri<sup>a</sup>, M. Raghunathan<sup>b</sup>, N. Rivals<sup>a</sup>, F. Schwander<sup>c</sup>, E. Serre<sup>c</sup>, S. Sureshkumar<sup>a</sup>, P. Tamain<sup>a</sup>, N. Varadarajan<sup>a</sup>

<sup>a</sup>CEA-IRFM, Cadarache, Saint-Paul-Lez-Durance, France

<sup>b</sup>Aix-Marseille Univ, CNRS, PIIM, Marseille, France

<sup>c</sup>Aix-Marseille Univ, CNRS, Centrale Med, M2P2, Marseille, France

## ARTICLE INFO

### Keywords:

Edge plasma  
Turbulence  
Modelling  
Plasma-wall interaction

## ABSTRACT

First principle modelling of edge plasma turbulence including neutrals and plasma recycling on the wall remains a challenge, in particular due to the long time scales necessary to simulate to reach particle balance. In this contribution, we propose a strategy to address these long time scales with the fluid code SOLEDGE3X, resorting to 2D reduced models for turbulence as well as 3D coarse grid simulations. The approach is applied to simulate TCV-X21 reference plasma scenario for edge turbulence modelling validation.

## 1. Introduction

Accurate modelling of cross-field turbulent transport in tokamak's edge plasma remains a challenge, many key experimental features such as edge transport barriers formation being still hard to simulate, especially for ITER size tokamaks. Being able to predict the SOL width or the power load imbalance between inner and outer divertor legs even for today's JET size tokamaks is still an open issue. First principle modelling of edge plasma turbulence is thus today a very active topic in the fusion community. A dedicated effort has been made in the scope of Eurofusion "Theory, Simulation, Verification and Validation" tasks to develop the codes and also to compare and confront the modelling results with experimental data. A typical example of this work is the TCV-X21 case [1] where a series of diverted ohmic L-mode discharges on TCV (Tokamak a Configuration Variable) were designed as a dataset for edge turbulence codes validation. The discharges were run in particular at low magnetic field to increase  $\rho^* = \rho_L/a$  and thus helping for the mesh grid resolution (typical mesh size being the Larmor radius  $\rho_L$ ). The experiments also targeted "sheath limited" conditions by operating at low density to minimize the impact of neutrals. The experimental data are publicly available for any code validation (<https://github.com/SPCData/TCV-X21>). In the pioneering Ref. [1], three European edge turbulence codes were benchmarked: GBS [2], GRILLIX [3] and TOKAM3X [4]. In that seminal work, simulations were run without neutral recycling and for numerical reasons, GBS and TOKAM3X had to reduce artificially heat and/or electrical

conductivity. Despite these simplifications, all codes recovered qualitatively the main Scrape-off Layer properties at the outboard midplane. However, significant discrepancies could be observed in the divertor area and on the divertor targets, the main suspects to explain these discrepancies being implementation of sheath boundary conditions and lack of neutral recycling.

A dedicated effort is now made in the community to take neutrals and plasma recycling into account in turbulent simulations [5–7]. In this contribution, we report on progress made to simulate TCV-X21 cases including neutral recycling with the SOLEDGE3X code [8,9] (successor of TOKAM3X) developed at CEA-IRFM and Aix-Marseille Université. Due to progress in numerical scheme and computing parallelization, TCV-X21 simulations could be run at full scale and with realistic heat and electric conductivities. Also, SOLEDGE3X implements several neutral models to address plasma recycling, from simple fluid models to a full kinetic description thanks to a coupling with EIRENE [10]. Section 2 details the simulation model and setup for the TCV-X21 case we consider. Then, Section 3 discusses the time scales to address and the subsequent challenges for the modelling. Finally, Section 4 focuses on divertor turbulence features observed in the modelling and comparison with experimental observations.

## 2. The SOLEDGE3X simulation setup

This section summarizes the key SOLEDGE3X features that have been used to simulate the TCV-X21 case with a special focus on the

\* Corresponding author.

E-mail address: [hugo.bufferand@cea.fr](mailto:hugo.bufferand@cea.fr) (H. Bufferand).

neutral model which is the key physical ingredient that has been added to the code since the TOKAM3X simulations presented in [1]. For more details on the plasma multi-component model implemented in SOLEDGE3X, please refer to [8].

### 2.1. The SOLEDGE3X fluid neutral models

The SOLEDGE3X code has been developed in the last five years, merging previous SOLEDGE2D and TOKAM3X codes. SOLEDGE3X relies on the drift-fluid approach and is able to cope with complex multi-component plasmas. Simulations can be run in 2D (axisymmetry) or 3D. Cross-field transport coefficients for particles  $D_{\perp}$ , momentum  $v_{\perp}$  and heat  $\chi_{\perp}$  can be set at:

- “classical values” (typically  $D_{\perp} \sim v_{\perp} \sim \chi_{\perp} \approx 10^{-2} \text{ m}^2 \text{ s}^{-1}$ ) for “first principle” turbulent simulations,
- “anomalous values” (typically  $D_{\perp} \sim v_{\perp} \sim \chi_{\perp} \approx 1 \text{ m}^2 \text{ s}^{-1}$ ) to emulate turbulence for transport simulations.

The code implements two main fluid models for plasma recycling and fuelling:

- Fluid neutrals, based on [11],
- Kinetic neutrals via a coupling with the EIRENE code.

The code is routinely run with EIRENE when used in 2D transport mode [12]. However, finely resolved 3D cases required for turbulence study remain undoable due to memory issues associated to the current parallelization of EIRENE. As a consequence, the fluid neutral description remains the main workhorse for SOLEDGE3X 3D turbulent simulations. In details, the fluid neutral implemented so far in SOLEDGE3X is the simplest version of the models proposed by [11]. Only atoms are taken into account (no molecules or molecular ions) and only neutral particle balance is considered:

$$\partial_t n_n + \vec{\nabla} \cdot (n_n \vec{v}_n) = -n_n n_e \langle \sigma v \rangle_{iz} + n_i n_e \langle \sigma v \rangle_{rec} + S_n \quad (1)$$

where  $n_n$  and  $\vec{v}_n$  denote neutral density and velocity,  $n_e$  and  $n_i$  denote electron and ion densities,  $\langle \sigma v \rangle_{iz}$  and  $\langle \sigma v \rangle_{rec}$  denote ionization and recombination cross sections and  $S_n$  denotes the source of atoms by recycling localized on the wall. The atoms velocity is computed from atoms momentum balance, neglecting inertia, and thus keeping only a static force balance between pressure force, charge exchange and ionization/recombination contribution, giving:

$$\begin{aligned} \partial_t m_n n_n \vec{v}_n + \vec{\nabla} \cdot (m_n n_n \vec{v}_n \vec{v}_n) = \\ -\vec{\nabla} p_n - m_n n_n n_e \vec{v}_n \langle \sigma v \rangle_{iz} + m_n n_i n_e \vec{v}_i \langle \sigma v \rangle_{rec} \\ - m_n n_n n_i \langle \sigma v \rangle_{CX} (\vec{v}_n - \vec{v}_i) \end{aligned} \quad (2)$$

This gives an algebraic expression for the atoms particle flux  $n_n \vec{v}_n$ :

$$n_n \vec{v}_n = -D_n \vec{\nabla} p_n + n_{n,eq} \vec{v}_i \quad (3)$$

with a quasi-diffusive part driven by the pressure gradient and where

$$D_n = \frac{1}{m_n (n_i \langle \sigma v \rangle_{CX} + n_e \langle \sigma v \rangle_{iz})} \quad (4)$$

and with a quasi-convective part driven by ions velocity where

$$n_{n,eq} = n_i \frac{n_n \langle \sigma v \rangle_{CX} + n_e \langle \sigma v \rangle_{rec}}{n_i \langle \sigma v \rangle_{CX} + n_e \langle \sigma v \rangle_{iz}} \quad (5)$$

Finally, since the energy balance is not solved for atoms, one assumes  $p_n = n_n T_n \approx n_n T_i$ . This fluid model can be improved step by step by solving the higher moments equations (first momentum balance and then energy balance) instead of doing the above mentioned approximations [13]. Concerning boundary conditions on the wall, one assumes a perfect reflection of atoms on the wall (zero net flux of atoms on the wall). A neutral source  $S_n$  is added on the wall to represent the atoms source by recycling. The source  $S_n$  is such as to reinject a fraction  $R_n$  of the incident plasma flux on the wall,  $R_n$  being the so-called recycling coefficient.

**Table 1**

Main plasma characteristics for TCV#51333, representative of TCV-X21 experiment conditions.

Parameter	Value
$R$	0.88 m
$a$	0.25 m
$B_{\phi}$	0.95 T
$I_p$	165 kA
$q_{95}$	3.2
$f_{GW}$	0.25
$P_{Ohm}$	150 kW

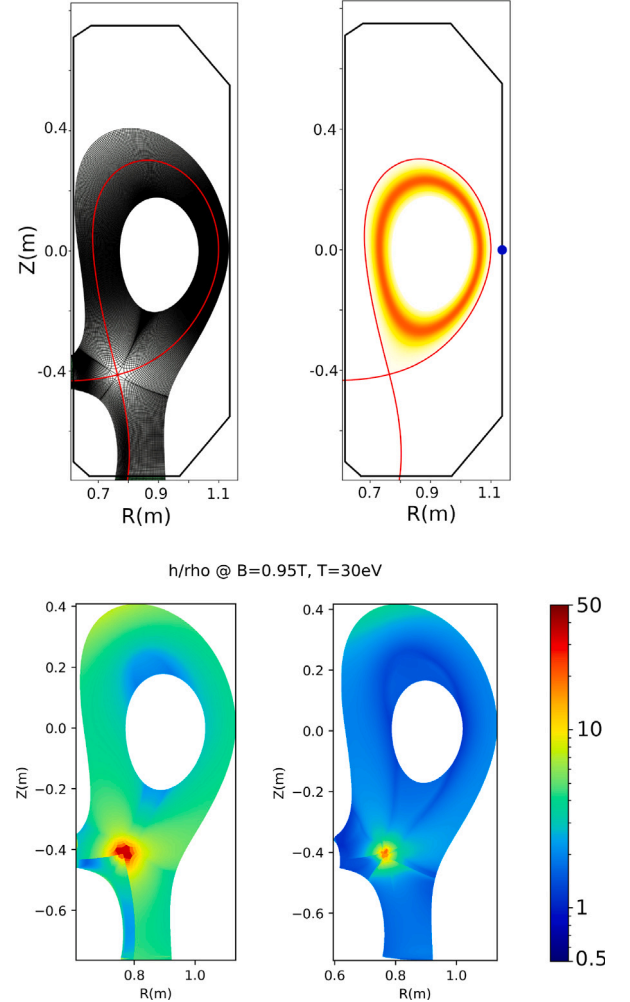


**Fig. 1.** Top left: coarse grid mesh. Top right: position of the heat source (orange) and gas puff (blue dot at the outboard mid-plane). Bottom left: coarse grid resolution in Larmor radius. Bottom right: fine grid resolution in term of Larmor radius. (For interpretation of the references to colour in this figure legend, the reader is referred to the web version of this article.)

### 2.2. Simulation setup for the TCV-X21 case

Different SOLEDGE3X grids were generated for TCV shot number 51333 from the TCV-X21 list of shots. TCV #51333 is a lower single null, L-mode Ohmic plasma. The toroidal field on axis is  $B_{\phi} = 0.95$  T. Other main characteristics are summarized in Table 1.

Fig. 1 shows TCV#51333 separatrix and vessel. Two grids were generated: a coarse grid with a poloidal resolution of about 4 mm (Grid 1) and a fine grid with a poloidal resolution of about 2 mm (Grid 2). The SOLEDGE3X grids are structured and aligned on magnetic flux surfaces using a domain decomposition to treat the X-point magnetic

**Table 2**  
Characteristics of SOLEDGE3X grids for TCV-X21.

	Grid1	Grid2	Grid3
Dimension	3D	3D	2D
Resolution	coarse	fine	coarse
$N_\phi$	32	64	1
$N_\theta$ (main SOL)	700	1300	700
$N_w$ (midplane)	100	220	100
$N_{points}$	2e6	1.7e7	6.2e4

topology. The coarse grid can also be used in 2D to perform transport simulation (Grid 3). The coarse grid is shown on Fig. 1 as well as the local grid resolution computed as the ratio between the longest mesh element edge length divided by a typical ion Larmor radius (computed for  $B = 0.95$  T and for a temperature of 30 eV, giving  $\rho_L \approx 0.9$  mm). For 3D cases, one simulates a quarter of the full torus ( $\Delta\phi = \pi/2$ ). The three grids characteristics are summarized in Table 2, in particular the typical number of points in each direction and the total number of points.

The simulation domain does not cover the entire TCV poloidal cross-section. The very core is not simulated as well as the far-SOL up to the first wall. The simulation domains lies between two flux surfaces, one in the core (or Private flux region), one in the Scrape-off layer. This volume restriction is done to reduce the number of points in the simulation domain. Wall boundary conditions (Bohm–Chodura for the plasma, reflective for neutrals) are applied at the boundary of this volume. As a consequence, the divertor in the simulation is less open than it is in reality in TCV.

The simulation is flux-driven and set by an energy source localized in the closed field line region (about  $r/a = 0.7$ ), see Fig. 1. The value of the source is set to  $P = 120$  kW shared equally between ions and electrons, 120 kW being an estimation of the power crossing separatrix for TCV-X21 cases (Ohmic power  $P_{Ohm} = 150$  kW from which is subtracted the power radiated in the core  $P_{rad,bulk} = 30$  kW). A gas puff localized at the outboard midplane also sets the plasma density at the separatrix by a feedback loop. One considers a pure Deuterium plasma and the recycling coefficient on the wall is set to  $R_n = 0.9$ . The value is quite low – even for a Carbon machine – and is expected to compensate for the closure of the divertor. In addition, a reduced recycling coefficient is expected to help converging simulation (see Section 3 below).

In addition, the following settings are used for cross-field diffusivities  $D_\perp$ ,  $\nu_\perp$ ,  $\chi_{\perp,e}$  and  $\chi_{\perp,i}$  denoting particle diffusivity, perpendicular viscosity, electrons and ions perpendicular heat conductivities respectively:

- for “first principle” turbulent simulations, all cross-field diffusivities are set to a classical level:

$$D_\perp = \nu_\perp = \chi_{\perp,e} = \chi_{\perp,i} = 10^{-2} \text{ m}^2\text{s}^{-1} \quad (6)$$

- for transport simulation, cross-field diffusivities are predicted by a  $k$ -model where  $k$  denotes turbulence kinetic energy. An equation for  $k$  is solved based on the semi-empirical turbulence reduced model described in [14].

### 3. Convergence and time scales

The main challenge when modelling edge plasma turbulence with neutral recycling is the range of time scales involved to reach a quasi-steady-state (QSS). Indeed, the following times scales must be addressed. First, the time scale associated with turbulence itself,  $\tau_{turb}$ , which is the time it takes for turbulent structures to develop given a fixed drive (density gradient, temperature gradient...). This time is quite fast and can be estimated for instance from interchange growth rate [15],  $\gamma = \tau_{turb}^{-1} = c_s(aR)^{-1/2}$ , giving  $\tau_{turb} \sim 10 \mu\text{s}$  for typical TCV-X21 parameters. Then, the typical transport time scale which

is the time necessary for energy and particles to cross radially our simulation domain. This time is of order  $\tau_{transp} = \delta r^2/D$  where  $\delta r$  is the radial extent of the simulation domain and  $D$  is a typical turbulent diffusivity. For our TCV-X21 grids,  $\delta_r \approx 10$  cm and  $D \sim 1 \text{ m}^2\text{s}^{-1}$  giving  $\tau_{transp} \sim 10$  ms. Finally, the longest time scale we consider is the time to reach particle balance. Due to strong recycling of neutrals with the wall, particle reservoirs take time to balance each others and the time to reach particle balance and quasi-steady-state can be estimated by  $\tau_{QSS} = \tau_{Sn}/(1-R_n)$  where  $\tau_{Sn}$  is the plasma transport time between the particle source location and the wall (typically a fraction of  $\tau_{transp}$ ) and  $R_n$  denoting the recycling coefficient. On saturated walls, the recycling coefficient takes values close to 1 making the time to reach particle balance very long (up to several seconds). For our TCV-X21 case, we chose  $R_n = 0.9$  to help converging towards a quasi-steady-state in a hundred of milliseconds. Even in that low- $R_n$  case, several orders of magnitude of time scales must be addressed between the fast turbulence and the slow particle balance dynamics.

Finding a strategy to address this challenge of long time scale simulation is key for a proper comparison between turbulent simulation with neutrals and experimental data acquired during the QSS plasma plateau in experiments. The strategy will of course depend on the numerical performance of the codes. For TCV-X21 experiment, SOLEDGE3X was run first in transport mode (2D) on the coarse grid (Grid 3) to reach particle balance. In that case, turbulence is emulated by diffusion predicted with the reduced  $k$ -model. Simulation results in QSS are shown on Fig. 2. The numerical cost is very cheap since particle balance is reached in a few hours of computation on a single 48CPUs node. However, the fidelity of the reduced turbulence model is low and the simulation must now be taken to the high-fidelity “first principle” frame of 3D turbulent simulations.

Restarting from the 2D plasma obtained with the reduced model, a 3D turbulent simulation is run on the coarse grid (Grid 1). The diffusivity is now set at classical level and turbulent structures such as plasma filament appear once plasma gradients start to locally steepen. The simulation is run for several days on 32 nodes of 48CPUs until almost a hundred of milliseconds of plasma are simulated. The numerical cost is now 25kCPUh for one millisecond of plasma. Even if the simulation was restarted from a plasma where particle and energy balances were reached, it takes a significant plasma/computation time to retrieve these global balances with the turbulent simulation. In order to avoid simulating this quite long transient during which turbulent structures appear, artificial fluctuations could be seeded on top of the mean field plasma to help speeding up the convergence towards the quasi-steady state. Fig. 3 shows particle and energy balance for the 2D mean field phase and for the latter 3D turbulent phase. In term of computation time again, if the first 90 ms 2D mean field plasma took about 1.2kCPUh, the last 90 ms 3D turbulent plasma took about 2.25MCPUh!

In parallel, a simulation was run on the fine grid (Grid 2) to estimate the numerical cost and code parallel efficiency to deal with a large number of grid points. The simulation was run during almost two weeks on 3072 CPUs and 0.8 ms of turbulent plasma were produced, giving a numerical cost on the fine grid evaluated at 1.25MCPUh per millisecond of plasma. Numerical costs are summarized in Table 3. The high price for running on the fine grid makes it impossible to reach with a brute force approach the necessary plasma time to reach QSS. The strategy is thus to interpolate turbulent results obtained on the coarse grid onto the fine grid and restart from that point, hoping most of the turbulent transport was caught by the coarse grid simulation run up to QSS, and that fine turbulent structures modify only marginally the transport and plasma confinement.

### 4. Recovering divertor turbulence features

Even if the exploratory fine grid simulation has not reached quasi-steady state, the 0.8 ms plasma time scale is enough for turbulence

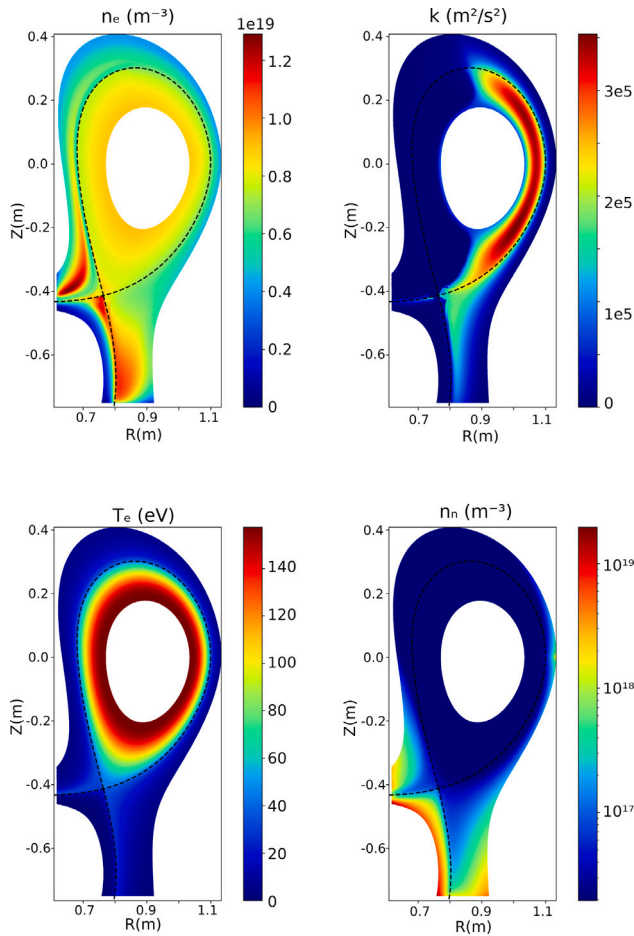


Fig. 2. Reduced turbulence model 2D simulation results at steady-state. Top left: electron density. Top right: turbulent kinetic energy. Bottom left: electron temperature. Bottom right: neutrals density.

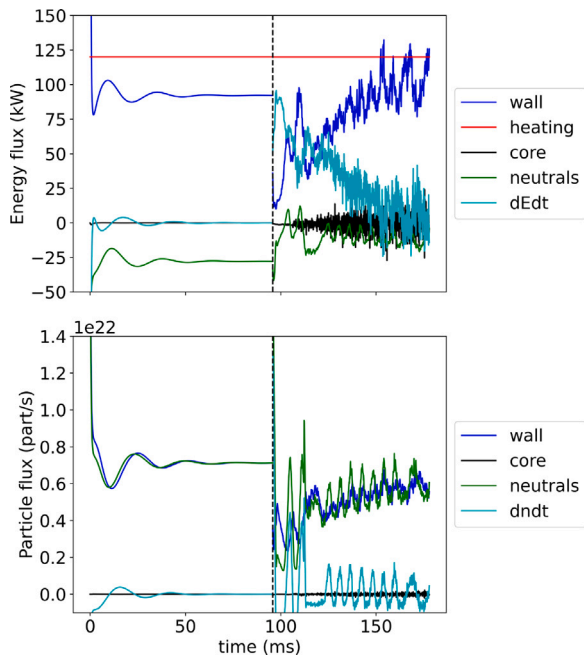


Fig. 3. Top: energy balance, bottom: particle balance. The first 90 ms are run in 2D mean field, the last 90 ms are run with 3D turbulence on the coarse grid.

Table 3

Numerical cost for solving 1 millisecond of plasma on the different grids considered.			
	Grid1	Grid2	Grid3
Dimension	3D	3D	2D
Resolution	coarse	fine	coarse
Cost (CPUh/ms)	25 000	1 250 000	13

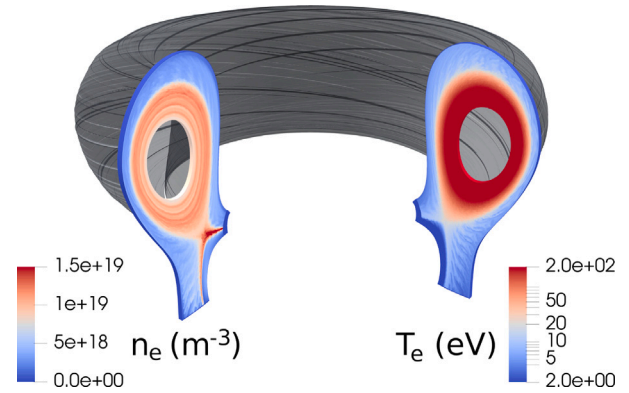


Fig. 4. 3D snapshot of SOLEDGE simulation results showing shape of turbulent filaments. Left poloidal plane shows electron density and right poloidal plane shows electron temperature.

to fully develop regarding the background free energy gradients. The shape and the dynamic of turbulence structures simulated can thus already be compared with experimental data, given that the initial density and pressure gradients were representative of the experimental plasma conditions. Fig. 4 illustrates typical simulation results, showing turbulent filaments as well as density and electron temperature in a given poloidal plane. Turbulent structures in the divertor are of particular interest and can be sorted in two categories:

- elongated filaments in the far scrape-off layer reminiscent from turbulent structures generated at the top of the plasma or at the outboard midplane and that are stretched by the flux expansion,
- small blobby structures localized along the divertor leg which are generated in the divertor and that characterize proper divertor turbulence which is decorrelated from the main plasma turbulence.

Both types of structures are carried by the mean ExB flow that tends to make elongated structures turning clockwise in the far scrape-off layer (towards the divertor plate for the outer leg) and the small blobby structures turning counter-clockwise (towards the X-point for the outer leg), see Fig. 5. This behaviour was also observed experimentally on TCV with gas puff imaging in [16] which characterizes so-called divertor localized filaments.

### 5. Conclusions

The first TCV-X21 turbulent simulations including plasma recycling with neutrals were run with the code SOLEDGE. The challenge to simulate long plasma time in turbulent regime to reach particle balance and quasi-steady state was addressed by a step by step approach, starting from a 2D mean field simulation that converges with a modest numerical cost to steady-state. The plasma obtained in 2D defines a good starting point for the more costly 3D turbulent simulation. Almost 100 ms of turbulent plasma were then simulated on a coarse grid. Ultimately, this coarse grid turbulent plasma should be used as a restart point on a more refined grid where small scale turbulent structures could be well resolved. If this procedure has not been used completely yet, first preliminary turbulent results on the fine grid with a fully developed turbulence recover key turbulent features observed

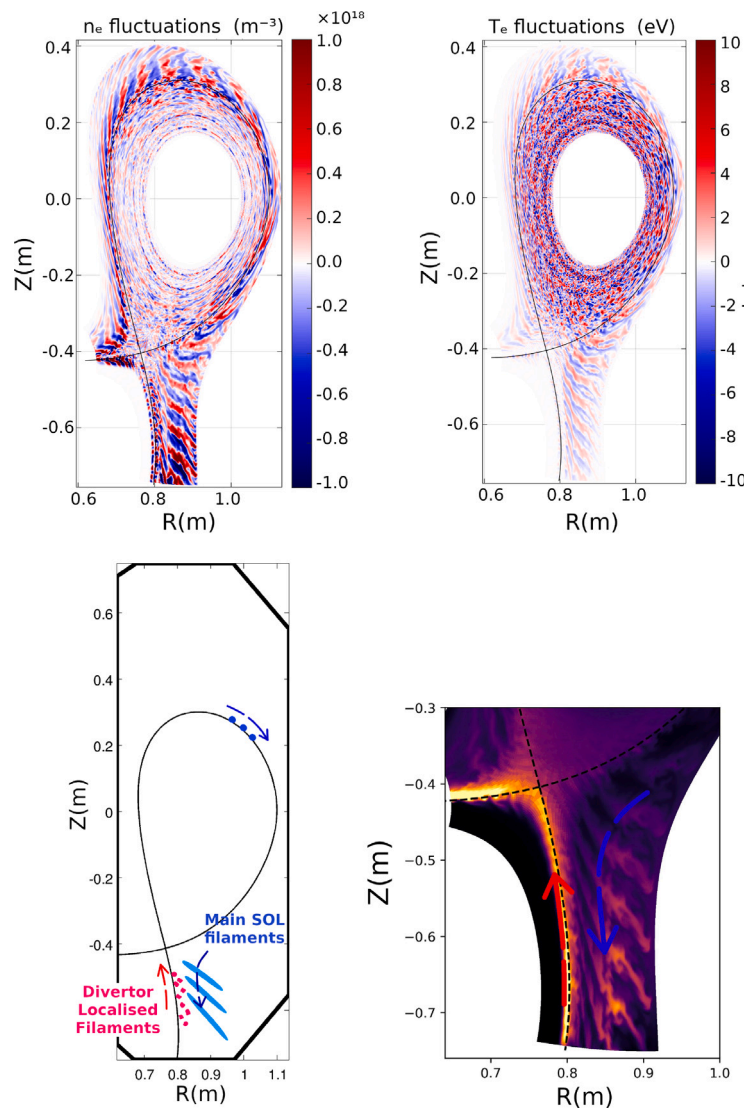


Fig. 5. Top row: Left: electron density fluctuations, Right: electron temperature fluctuations. Bottom row: Left: sketch of turbulence structures in TCV divertor showing divertor localized filaments. Right: neutrals radiation in the divertor (proxy for what could be visible with gas puff imaging diagnostic).

experimentally such as divertor localized filaments. A more detailed comparison with TCV-X21 experimental database should be carried out once QSS is reached on the finer grid.

#### CRedit authorship contribution statement

**H. Bufferand:** Writing – review & editing, Writing – original draft, Supervision, Software, Methodology, Investigation, Data curation, Conceptualization. **G. Ciraolo:** Supervision, Project administration, Methodology, Investigation. **R. Düll:** Software, Investigation. **G. Falchetto:** Methodology, Conceptualization. **N. Fedorcak:** Methodology, Formal analysis, Conceptualization. **Y. Marandet:** Software, Formal analysis. **V. Quadri:** Software, Data curation. **M. Raghunathan:** Formal analysis, Data curation. **N. Rivals:** Validation, Software. **F. Schwander:** Methodology, Conceptualization. **E. Serre:** Supervision, Methodology, Conceptualization. **S. Sureshkumar:** Software. **P. Tamain:** Validation, Software, Methodology. **N. Varadarajan:** Software.

#### Declaration of competing interest

The authors declare that they have no known competing financial interests or personal relationships that could have appeared to influence the work reported in this paper.

#### Acknowledgements

This work was granted access to the HPC/AI resources of CINES/IDRIS/TGCC under the allocation 2023-A0140510482 made by GENCI and the Grand Challenge ToDo on ADASTRA supercomputer. This work has been carried out within the framework of the EUROfusion Consortium, funded by the European Union via the Euratom Research and Training Programme (Grant Agreement No 101052200 — EUROfusion). Views and opinions expressed are however those of the author(s) only and do not necessarily reflect those of the European Union or the European Commission. Neither the European Union nor the European Commission can be held responsible for them.

#### Data availability

Data will be made available on request.

#### References

- [1] D. Oliveira, T. Body, D. Galassi, C. Theiler, E. Laribi, P. Tamain, A. Stegmeir, M. Giacomini, W. Zholobenko, P. Ricci, H. Bufferand, J. Boedo, G. Ciraolo, C. Colandrea, D. Coster, H. de Oliveira, G. Fourestey, S. Gorno, F. Imbeaux, F.

- Jenko, V. Naulin, N. Offeddu, H. Reimerdes, E. Serre, C. Tsui, N. Varini, N. Vianello, M. Wiesenberger, C. Wüthrich, the TCV Team, Validation of edge turbulence codes against the TCV-X21 diverted L-mode reference case, *Nucl. Fusion* 62 (9) (2022) 096001, <http://dx.doi.org/10.1088/1741-4326/ac4cde>, URL <http://dx.doi.org/10.1088/1741-4326/ac4cde>.
- [2] P. Ricci, F.D. Halpern, S. Jolliet, J. Loizu, A. Masetto, A. Fasoli, I. Furno, C. Theiler, Simulation of plasma turbulence in scrape-off layer conditions: the GBS code, simulation results and code validation, *Plasma Phys. Control. Fusion* 54 (12) (2012) 124047, <http://dx.doi.org/10.1088/0741-3335/54/12/124047>, URL <http://dx.doi.org/10.1088/0741-3335/54/12/124047>.
- [3] A. Stegmeir, A. Ross, T. Body, M. Francisquez, W. Zholobenko, D. Coster, O. Maj, P. Manz, F. Jenko, B.N. Rogers, K.S. Kang, Global turbulence simulations of the tokamak edge region with GRILLIX, *Phys. Plasmas* 26 (5) (2019) 052517, <http://dx.doi.org/10.1063/1.5089864>, URL <http://dx.doi.org/10.1063/1.5089864>.
- [4] P. Tamain, H. Bufferand, G. Ciraolo, C. Colin, D. Galassi, P. Ghendrih, F. Schwander, E. Serre, The TOKAM3X code for edge turbulence fluid simulations of tokamak plasmas in versatile magnetic geometries, *J. Comput. Phys.* 321 (2016) 606–623, <http://dx.doi.org/10.1016/j.jcp.2016.05.038>, URL <https://www.sciencedirect.com/science/article/pii/S0021999116301838>.
- [5] W. Zholobenko, A. Stegmeir, M. Griener, G. Conway, T. Body, D. Coster, F. Jenko, the ASDEX Upgrade Team, The role of neutral gas in validated global edge turbulence simulations, *Nucl. Fusion* 61 (11) (2021) 116015, <http://dx.doi.org/10.1088/1741-4326/ac1e61>, URL <http://dx.doi.org/10.1088/1741-4326/ac1e61>.
- [6] M. Giacomin, P. Ricci, A. Coroado, G. Fourestey, D. Galassi, E. Lanti, D. Mancini, N. Richart, L. Stenger, N. Varini, The GBS code for the self-consistent simulation of plasma turbulence and kinetic neutral dynamics in the tokamak boundary, *J. Comput. Phys.* 463 (2022) 111294, <http://dx.doi.org/10.1016/j.jcp.2022.111294>, URL <https://www.sciencedirect.com/science/article/pii/S0021999122003564>.
- [7] B. Dudson, M. Kryjak, H. Muhammed, P. Hill, J. Omotani, Hermes-3: Multi-component plasma simulations with BOUT++, *Comput. Phys. Comm.* 296 (2024) 108991, <http://dx.doi.org/10.1016/j.cpc.2023.108991>, URL <https://www.sciencedirect.com/science/article/pii/S0010465523003363>.
- [8] H. Bufferand, J. Bucalossi, G. Ciraolo, G. Falchetto, A. Gallo, P. Ghendrih, N. Rivals, P. Tamain, H. Yang, G. Giorgiani, F. Schwander, M.S. d'Abusco, E. Serre, Y. Marandet, M. Raghunathan, W. Team, the JET Team, Progress in edge plasma turbulence modelling—hierarchy of models from 2D transport application to 3D fluid simulations in realistic tokamak geometry, *Nucl. Fusion* 61 (11) (2021) 116052, <http://dx.doi.org/10.1088/1741-4326/ac2873>, URL <http://dx.doi.org/10.1088/1741-4326/ac2873>.
- [9] SOLEDGE3X, Soledge3x website, 2024, Accessed:(1October2024).
- [10] EIRENE, Eirene website, 2024, <https://eirene.de/> [Accessed: (1 October 2024)].
- [11] N. Horsten, G. Samaey, M. Baelmans, Development and assessment of 2D fluid neutral models that include atomic databases and a microscopic reflection model, *Nucl. Fusion* 57 (11) (2017) 116043, <http://dx.doi.org/10.1088/1741-4326/aa8009>, URL <http://dx.doi.org/10.1088/1741-4326/aa8009>.
- [12] N. Rivals, P. Tamain, Y. Marandet, X. Bonnin, H. Bufferand, R.A. Pitts, G. Falchetto, H. Yang, G. Ciraolo, SOLEDGE3X full vessel plasma simulations for computation of ITER first-wall fluxes, *Contrib. Plasma Phys.* 62 (5–6) (2022) e202100182, <http://dx.doi.org/10.1002/ctpp.202100182>, URL <https://onlinelibrary.wiley.com/doi/abs/10.1002/ctpp.202100182>.
- [13] W.V. Uytven, W. Dekeyser, M. Blommaert, S. Carli, M. Baelmans, Assessment of advanced fluid neutral models for the neutral atoms in the plasma edge and application in ITER geometry, *Nucl. Fusion* 62 (8) (2022) 086023, <http://dx.doi.org/10.1088/1741-4326/ac72b4>, URL <http://dx.doi.org/10.1088/1741-4326/ac72b4>.
- [14] S. Baschetti, H. Bufferand, G. Ciraolo, N. Fedorczak, P. Ghendrih, P. Tamain, E. Serre, A  $\kappa$ - $\epsilon$  model for plasma anomalous transport in tokamaks: closure via the scaling of the global confinement, *Nuclear Mater. Energy* 19 (2019) 200–204, <http://dx.doi.org/10.1016/j.nme.2019.02.032>, URL <https://www.sciencedirect.com/science/article/pii/S2352179118301996>.
- [15] R.J. Goldston, P.H. Rutherford, *Introduction to Plasma Physics*, Institute of Physics Pub, Bristol UK, 1995.
- [16] C. Wüthrich, C. Theiler, N. Offeddu, D. Galassi, D. Oliveira, B. Duval, O. Février, T. Golfopoulos, W. Han, E. Marmar, J. Terry, C. Tsui, the TCV Team, X-point and divertor filament dynamics from gas puff imaging on TCV, *Nucl. Fusion* 62 (10) (2022) 106022, <http://dx.doi.org/10.1088/1741-4326/ac8692>, URL <http://dx.doi.org/10.1088/1741-4326/ac8692>.